Upper limit of D^0 production in central Pb-Pb collisions at 158*A* GeV

C. Alt,[9] T. Anticic,[21] B. Baatar,[8] D. Barna,[4] J. Bartke,[6] L. Betev,[10] H. Białkowska,[19] C. Blume,[9] B. Boimska,[19] M. Botje,[1] J. Bracinik,[3] R. Bramm,[9] P. Buncic,[10] V. Cerny,[3] P. Christakoglou,[2] O. Chvala,[14] J. G. Cramer,[16] P. Csató,[4] P. Dinkelaker,[9] V. Eckardt,[13] D. Flierl,[9] Z. Fodor,[4] P. Foka,[7] V. Friese,[7] J. Gál,[4] M. Gaździcki,[9,11] V. Genchev,[18] G. Georgopoulos,[2] E. Gładysz,[6] K. Grebieszkow,[20] S. Hegyi,[4] C. Höhne,[7] K. Kadija,[21] A. Karev,[13] M. Kliemant,[9] S. Kniege,[9] V. I. Kolesnikov,[8] E. Kornas,[6] R. Korus,[11] M. Kowalski,[6] I. Kraus,[7] M. Kreps,[3] M. van Leeuwen,[1] P. Lévai,[4] L. Litov,[17] B. Lungwitz,[9] M. Makariev,[17] A. I. Malakhov,[8] C. Markert,[7] M. Mateev,[17] G. L. Melkumov,[8] A. Mischke,[1] M. Mitrovski,[9] J. Molnár,[4] St. Mrówczyński,[11] V. Nicolic,[21] G. Pálla,[4] A. D. Panagiotou,[2] D. Panayotov,[17] A. Petridis,[2] M. Pikna,[3] D. Prindle,[16] F. Pühlhofer,[12] R. Renfordt,[9] C. Roland,[5] G. Roland,[5] M. Rybczyński,[11] A. Rybicki,[6,10] A. Sandoval,[7] N. Schmitz,[13] T. Schuster,[9] P. Seyboth,[13] F. Siklér,[4] B. Sitar,[3] E. Skrzypczak,[20] G. Stefanek,[11] R. Stock,[9] H. Ströbele,[9] T. Susa,[21] I. Szentpétery,[4] J. Sziklai,[4] P. Szymanski,[10,19] V. Trubnikov,[19] D. Varga,[4,10] M. Vassiliou,[2] G. I. Veres,[4,5] G. Vesztergombi,[4] D. Vranić,[7] A. Wetzler,[9] Z. Włodarczyk,[11] I. K. Yoo,[15] and J. Zimányi[4]

(NA49 Collaboration)

[1]*NIKHEF, Amsterdam, Netherlands*

[2]*Department of Physics, University of Athens, Athens, Greece*

[3]*Comenius University, Bratislava, Slovakia*

[4]*KFKI Research Institute for Particle and Nuclear Physics, Budapest, Hungary*

[5]*MIT, Cambridge, Massachusetts USA*

[6]*Institute of Nuclear Physics, Cracow, Poland*

[7]*Gesellschaft für Schwerionenforschung (GSI), Darmstadt, Germany*

[8]*Joint Institute for Nuclear Research, Dubna, Russia*

[9]*Fachbereich Physik der Universität, Frankfurt, Germany*

[10]*CERN, Geneva, Switzerland*

[11]*Institute of Physics Świetokrzyska Academy, Kielce, Poland*

[12]*Fachbereich Physik der Universität, Marburg, Germany*

[13]*Max-Planck-Institut für Physik, Munich, Germany*

[14]*Institute of Particle and Nuclear Physics, Charles University, Prague, Czech Republic*

[15]*Department of Physics, Pusan National University, Pusan, Republic of Korea*

[16]*Nuclear Physics Laboratory, University of Washington, Seattle, Washington USA*

[17]*Atomic Physics Department, Sofia University St. Kliment Ohridski, Sofia, Bulgaria*

[18]*Institute for Nuclear Research and Nuclear Energy, Sofia, Bulgaria*

[19]*Institute for Nuclear Studies, Warsaw, Poland*

[20]*Institute for Experimental Physics, University of Warsaw, Warsaw, Poland*

[21]*Rudjer Boskovic Institute, Zagreb, Croatia*

(Received 27 July 2005; published 22 March 2006)

Results are presented from a search for the decays $D^0 \to K^-\pi^+$ and $\bar{D}^0 \to K^+\pi^-$ in a sample of 3.8×10^6 central Pb-Pb events collected with a beam energy of 158*A* GeV by NA49 at the CERN SPS. No signal is observed. An upper limit on D^0 production is derived and compared to predictions from several models.

DOI: 10.1103/PhysRevC.73.034910 PACS number(s): 25.75.Dw

The measurement of open charm production in heavy-ion interactions is of considerable interest because charm, due to its large mass, is predominantly created at the early stage of the collision when the energy density is large. Because of the hard scale involved, perturbative QCD (pQCD) calculations can serve as a baseline for the study of the production mechanisms and the dynamical evolution of charm in these collisions.

At present, no direct measurement exists of open charm production in heavy-ion interactions at SPS energies. The NA38/50 experiment has, however, observed a significant enhancement of dimuon production in the intermediate mass range of 1.5–2.5 GeV, compared to dimuon yields expected from the Drell-Yan continuum and semi-leptonic charm decays [1]. The origin of this enhancement is presently not clear but can be explained by assuming that open charm production in central Pb-Pb collisions is about a factor of 3.5 times larger than predicted by pQCD. This enhancement is currently under investigation by the NA60 experiment [2].

A variety of models give very different estimates for the open charm yields at the SPS. For instance, for central Pb-Pb interactions at 158*A* GeV beam energy, a pQCD calculation based on PYTHIA predicts a yield per event of $N(D^0 + \bar{D}^0) = 0.21$ (the centrality is here characterized by the number of participant nucleons $N_{\text{part}} = 400$) [3]. In Ref. [4], a yield of 0.5–0.6 $c\bar{c}$ quark pairs is calculated, based on the J/Ψ yield measured by NA50 and the statistical coalescence model ($N_{\text{part}} = 360$). This translates into $N(D^0 + \bar{D}^0) \approx 0.4$ if one assumes that about one-third of the $c\bar{c}$ hadronize into D^0 and

$\bar{D}^0$, like in *p-p* interactions [5]. The ALCOR hadronization model [6] gives a much larger estimate of $N(D^0 + \bar{D}^0) = 2.4$ ($N_{\text{part}} \approx 350$). An even larger yield of $N(D^0 + \bar{D}^0) \approx 6$ is predicted by the statistical model of the early stage (SMES) which assumes charm equilibration in a deconfined quark-gluon plasma (QGP) at the early stage of the Pb-Pb interaction ($N_{\text{part}} = 360$) [7].

To discriminate between the different model predictions and to possibly identify the origin of the dimuon enhancement seen by NA38/50, we have performed a search for open charm, using invariant mass reconstruction, in a large data sample of about 4×10^6 central Pb-Pb events collected at 158*A* GeV beam energy.

The NA49 detector [8] is a large acceptance fixed-target hadron spectrometer at the CERN SPS. Tracking is performed by four large-volume TPCs. Two of these are placed one behind the other inside two super-conducting dipole magnets (vertex TPCs). The two other (main) TPCs are placed downstream of the magnets left and right of the beam line. These main TPCs increase the lever arm of the track reconstruction and are optimized for particle identification through a measurement of the specific energy loss (dE/dx) with a relative resolution of about 4%. The combined TPCs provide an accurate measurement of the particle momenta with a resolution of $\Delta p/p^2 \approx 3 \times 10^{-5}$ (GeV/c)$^{-1}$. Centrality selection is based on a measurement of the energy deposited by the projectile spectator nucleons in a forward calorimeter.

To measure rare particles like the Ω [9] and to search for open charm a large sample of central Pb-Pb events was taken in the year 2000 with a beam energy of 158*A* GeV. In this run 3×10^6 events were collected with a centrality selection of 23.5% of the inelastic cross section ($N_{\text{part}} = 262$). Also included in the present analysis is a 1996 data set of 8×10^5 Pb-Pb events, taken at the same beam energy but with a 10% centrality selection ($N_{\text{part}} = 335$). To increase the data acquisition speed and decrease the data volume only every second time-sample of the TPCs was read out during the 2000 run (256 instead of 512 time-samples). The reduced sampling did not significantly affect the track reconstruction nor the dE/dx measurement.

The D^0 were reconstructed via their charged particle decays $D^0 \to K^-\pi^+$ and $\bar{D}^0 \to K^+\pi^-$ (4% branching ratio). Because the secondary vertex resolution of about 1 cm is not sufficient to detect the decay vertex ($\gamma c\tau \approx 1$ mm), the D^0 candidates were identified by selecting a window around the D^0 mass in the invariant mass spectrum of the daughter particles. With a multiplicity of approximately 1400 reconstructed charged tracks, about 5×10^5 entries for each event were made in each of the D^0 and $\bar{D}^0$ invariant mass spectra leading to a large combinatorial background. Because of the large multiplicities it was not possible to measure the three-particle decay $D^* \to K\pi\pi$ even though the background in this channel is suppressed by kinematic constraints.

Events for which the primary vertex could not be determined were discarded from the analysis. Several track quality cuts [10] were applied to remove nonvertex or badly reconstructed tracks. The remaining sample was subdivided into two classes. The tracks in the first class have sufficient track length in the main TPCs and low enough momentum

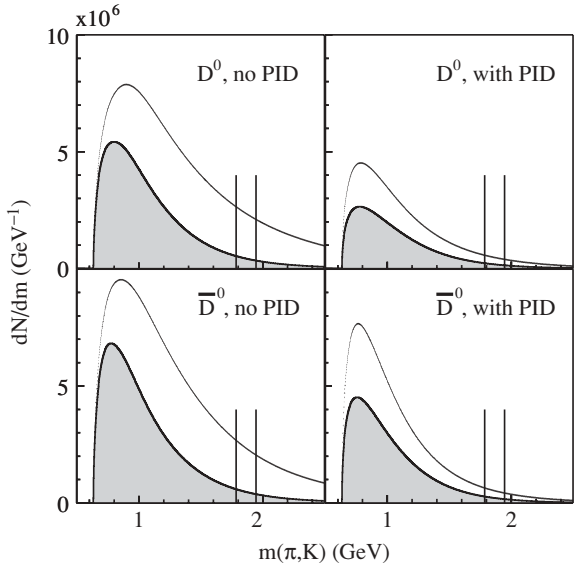

FIG. 1. Invariant mass distributions of D^0 (top) and $\bar{D}^0$ candidates (bottom) from track samples without (left) and with (right) kaon identification. The open (shaded) histograms are before (after) applying the decay angle cuts described in the text. The vertical lines indicate the D^0 mass window used in the analysis. The distributions are corrected for acceptance and branching ratio.

so that a significant enrichment of the kaon content could be achieved by suitable cuts on dE/dx. For tracks in the second class this kaon identification was not possible. Loose cuts on dE/dx (2σ around the Bethe-Bloch curve) were applied on the tracks in the first sample to minimize the loss of kaons (and D^0). The identified kaon tracks were then combined with all oppositely charged tracks and the invariant mass of the pair was calculated assuming that the associated track was a pion. In the second class (without dE/dx) the invariant mass of the D^0 ($\bar{D}^0$) candidate was calculated for all pairs of oppositely charged tracks assuming that the positive track was a pion (kaon) and the negative track a kaon (pion). The invariant mass distributions obtained from the D^0 and $\bar{D}^0$ samples with and without kaon identification (corrected for acceptance and efficiency, see below) are shown by the open histograms in Fig. 1.

To further reduce the combinatorial background, decay angle cuts were applied as follows. For each D^0 candidate the polar angle θ and the azimuthal angle ϕ of the kaon track were calculated in the rest-frame of the D^0. Here θ is the angle between the beam direction and the kaon flight direction and ϕ the angle between the kaon and the flight direction of the D^0 in the plane perpendicular to the beam. In the left-hand side plot of Fig. 2 is shown the distribution of decay angles from simulated D^0 decays (see below). The distribution from real events (almost entirely background) is shown in the right-hand side plot. It is clear from this figure that the signal distribution is approximately flat while the background distribution peaks at large values of $|\cos\theta|$. Cuts, like those shown in the figure, were optimized to maximize the significance ($= \text{signal}/\sqrt{\text{background}}$) of the measurement. Because the decay angle distribution depends on the transverse

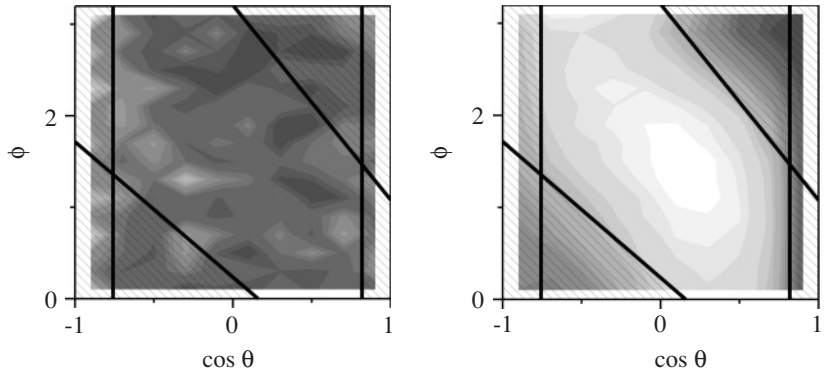

FIG. 2. The reconstructed decay angle distributions (see text) of simulated D^0 decays (left) and of D^0 candidates from real events (right). In both plots the D^0 candidates have a reconstructed mass within 50 MeV of the nominal D^0 mass and a reconstructed p_T of 800–1200 MeV. A darker shade corresponds to more entries in the plots. The full lines indicate the cuts used in the analysis to discard the hatched regions.

momentum (p_T) of the D^0 and is different for the samples with and without particle identification, separate cuts were determined, for each of the two samples, in five p_T bins of 400 MeV width. The decay angle cuts reduced the background by a factor of about 3 (10) in the sample with (without) particle identification. (The signal is reduced by 30%–40%.) Cuts on other kinematic variables like rapidity (y) and p_T were investigated but were found to be ineffective in the separation of signal and background [10]. The invariant mass distributions after the decay angle cuts and corrected for acceptance and efficiency (see below) are shown by the shaded histograms in Fig. 1.

To determine acceptance, efficiency and mass resolution a Monte Carlo sample of D^0 and $\bar{D}^0$ mesons was generated with a Gaussian distribution in y ($\sigma_y = 0.6$) and an exponential distribution in transverse mass (300 MeV inverse slope parameter). The D^0 ($\bar{D}^0$) and their decay particles were transported through the NA49 detector geometry using GEANT 3.21 [11], followed by a detailed simulation of the TPC response using dedicated NA49 software. The simulated raw data were added to real events and subjected to the same reconstruction procedure as the experimental data. The acceptance was calculated in bins of y and p_T as the fraction of D^0 ($\bar{D}^0$) which are geometrically accepted, survive the reconstruction procedure and pass the analysis cuts. The experimental acceptance covers the range $p_T > 0$ and $-1 \lesssim y \lesssim 1.6$ and is found to be, on average, 8.4 (12.0)% for the sample with (without) kaon identification. It was verified that the amount of accepted particles varied by only 10–20% if reasonable alternatives (e.g., from PYTHIA [12]) were chosen for the kinematic distribution of the D^0. The invariant mass distributions shown in Fig. 1 are divided by the acceptance and by the branching ratio for $D \to \pi K$ decay.

The simulated data served to determine the shape of the invariant mass distribution of reconstructed D^0 as shown in Fig. 3. The shape can be well described by a Cauchy distribution (curve in Fig. 3)

$$\frac{dn}{dm} = \frac{N}{2\pi} \frac{\Gamma}{(m - m_0)^2 + (\Gamma/2)^2}, \qquad (1)$$

where N is the total D^0 yield per event, m_0 the D^0 mass and Γ the width of the distribution. This width is almost entirely determined by the detector resolution and is found to be $\Gamma = 6.2$ MeV with the mass of the D^0 set to $m_0 = 1864.5$ MeV [13].

The invariant mass spectra obtained after decay angle cuts with and without kaon identification (Fig. 1) were added together for D^0 and $\bar{D}^0$ separately. The resulting spectra were fitted (by χ^2 minimization) in a region of ± 90 MeV around the nominal D^0 mass to the sum of a signal distribution, Eq. (1), and a fourth order polynomial describing the background. The position m_0 and width Γ of the signal distribution were kept fixed to the values given above while the normalization N was left a free parameter in the fit. This fit results in yields (per event) of $N(D^0) = -0.41 \pm 0.51$ and $N(\bar{D}^0) = 0.05 \pm 0.54$, where the errors are statistical only. In Fig. 4 is shown the invariant mass distribution of the $D^0 + \bar{D}^0$ candidates after background subtraction. Clearly no signal is observed. The fit gave for the total yield a value of $N(D^0 + \bar{D}^0) = -0.36 \pm 0.74$ per event (full line in Fig. 4).

An upper limit for the number of D^0 per event is estimated in a Bayesian approach [14]. Here the likelihood $P(\text{data}|N)$ (i.e., the conditional probability density distribution of the data, given N D^0 per event) is parametrized as a Gaussian

$$P(\text{data}|N) = \frac{1}{\sigma\sqrt{2\pi}} \exp\left[-\frac{(N-\mu)^2}{2\sigma^2}\right] \equiv g(N; \mu, \sigma) \qquad (2)$$

with mean $\mu = -0.36$ and width $\sigma = 0.74$ as obtained from the χ^2 fit. Using Bayes' theorem the posterior distribution $P(N|\text{data})$ is calculated by multiplying the likelihood with an assumed prior probability distribution of N which is taken here to be zero for $N < 0$ and uniform for $N \geqslant 0$. This prior

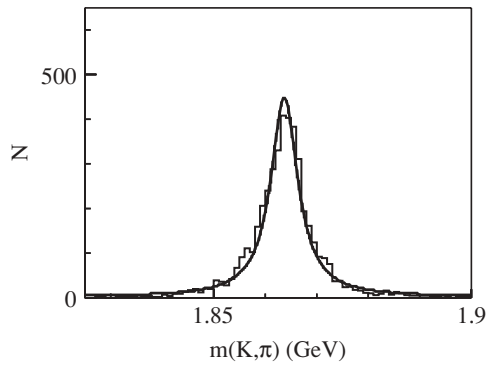

FIG. 3. Invariant mass distribution of simulated D^0 decays embedded in real data events. The full curve shows the Cauchy parametrization described in the text.

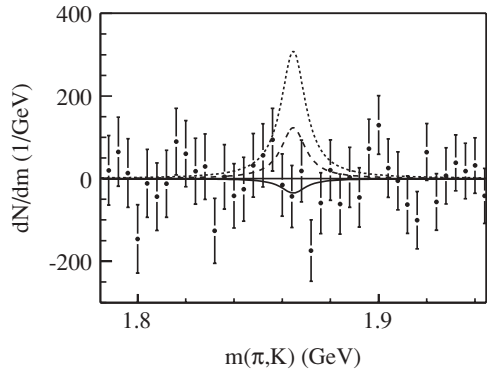

FIG. 4. Invariant mass distribution of the $D^0+\bar{D}^0$ candidates after background subtraction. The errors are statistical only. The full curve shows the fit to the signal distribution described in the text, the dashed curve the expectation from ALCOR [6] and the dotted curve that from SMES [7].

distribution forces N to be positive, as it should be. Integration of the posterior distribution gives for the confidence level

$$\mathrm{CL} \equiv \int_0^M P(N|\mathrm{data})\,dN = \frac{\int_0^M g(N;\mu,\sigma)\,dN}{\int_0^\infty g(N;\mu,\sigma)\,dN}, \qquad (3)$$

where M is the upper limit of N corresponding to the confidence level CL. The denominator on the right-hand side of Eq. (3) accounts for the proper normalization of $P(N|\mathrm{data})$. Using the fitted values of μ and σ, the upper limit for the total yield is found to be $M(D^0+\bar{D}^0) = 1.5$ per event at 98% CL.

Because no D^0 signal has been observed it is not possible to directly verify the Monte Carlo prediction of the signal shape. To investigate the sensitivity of the upper limit to the width of the mass peak the fits were repeated with $\Gamma = 12.4$ MeV. This resulted in $N(D^0) = -0.46 \pm 0.85$, $N(\bar{D}^0) = -0.22 \pm 0.90$, $N(D^0+\bar{D}^0) = -0.7 \pm 1.2$ and an upper limit of $M(D^0+\bar{D}^0) = 2.4$ per event at 98% CL. We remark that increasing the Monte Carlo estimate of the width by a factor of two should be considered a very generous error on Γ.

We conclude that our upper limit $M(D^0+\bar{D}^0) = 1.5$ per event is consistent with the pQCD estimate of 0.21 mentioned in the introduction. Thus a large enhancement of charm production in Pb-Pb collisions at SPS energies appears unlikely. Consistency with pQCD calculations was also found for Au-Au reactions at RHIC [15]. Due to the large combinatorial background it is not possible to confirm, nor exclude, a charm enhancement by a factor of three allowed by the NA38/50 measurement. However, the D^0 upper limit from this analysis is only marginally compatible with the yield estimated by the ALCOR model (dashed curve in Fig. 4) and clearly incompatible with the equilibrium yield of charm in a QGP as predicted by the SMES (dotted curve in Fig. 4). The latter observation does not necessarily exclude QGP formation at SPS energies provided that the QGP lifetime is shorter than the equilibration time of charm.

ACKNOWLEDGMENTS

This work was supported by the U.S. Department of Energy Grant No. DE-FG03-97ER41020/A000, the Bundesministerium fur Bildung und Forschung, Germany, the Virtual Institute VI-146 of Helmholtz Gemeinschaft, Germany, the Polish State Committee for Scientific Research (2 P03B 130 23, SPB/CERN/P-03/Dz 446/2002-2004, 2 P03B 04123), the Hungarian Scientific Research Foundation (T032648, T032293, T043514), the Hungarian National Science Foundation, OTKA, (F034707), the Polish-German Foundation, and the Korea Research Foundation Grant (KRF-2003-070-C00015).

[1] M. C. Abreu *et al.* (NA38 and NA50 Collaboration), Eur. Phys. J. C **14**, 443 (2000).
[2] A. Baldit *et al.* (NA60 Collaboration), CERN/SPSC-2000-010 (2000).
[3] P. Braun-Munziger *et al.*, Eur. Phys. J. C **1**, 123 (1998); P. Braun-Munziger and J. Stachel, Phys. Lett. **B490**, 196 (2000).
[4] M. I. Gorenstein *et al.*, Phys. Lett. **B509**, 277 (2001).
[5] M. Aguilar-Benitez *et al.* (LEBC-EHS Collaboration), Z. Phys. C **40**, 321 (1988).
[6] P. Lévai *et al.*, J. Phys. G **27**, 703 (2001).
[7] M. Gaździcki and M. I. Gorenstein, Acta Phys. Pol. B **30**, 2705 (1999); M. Gaździcki and C. Markert, *ibid.* **31**, 965 (2000).
[8] S. Afanasiev *et al.* (NA49 Collaboration), Nucl. Instrum. Methods A **430**, 210 (1999).
[9] C. Alt *et al.* (NA49 Collaboration), Phys. Rev. Lett. **94**, 192301 (2005).
[10] M. van Leeuwen, Ph.D. thesis, University of Utrecht, 2003, available from http://na49info.cern.ch
[11] R. Brun *et al.*, GEANT User Guide and Reference Manual, CERN-DD-78-2-REV (1978).
[12] T. Sjöstrand *et al.*, Comput. Phys. Commun. **135**, 238 (2001).
[13] K. Hagiwara *et al.* (Particle Data Group), Phys. Rev. D **66**, 010001 (2002).
[14] D. S. Sivia, *Data Analysis—a Bayesian Tutorial* (Oxford University Press, Oxford, 1997).
[15] K. Adcox *et al.* (PHENIX Collaboration), Phys. Rev. Lett. **88**, 192303 (2002); S. S. Adler *et al.* (PHENIX Collaboration), *ibid.* **94**, 082301 (2005).